SPECIAL TOPIC — Active matters physics

Constraint dependence of average potential energy of a passive particle in an active bath*

Simin Ye(叶思敏)[1,2,†], Peng Liu(刘鹏)[1,2,†], Zixuan Wei(魏子轩)[2], Fangfu Ye(叶方富)[1,2,3,4,‡], Mingcheng Yang(杨明成)[1,2,§], and Ke Chen(陈科)[1,2,3,¶]

[1] *Beijing National Laboratory for Condensed Matter Physics and Institute of Physics, Chinese Academy of Sciences, Beijing* 100190, *China*
[2] *School of Physical Sciences, University of Chinese Academy of Sciences, Beijing* 100049, *China*
[3] *Songshan Lake Materials Laboratory, Dongguan* 523808, *China*
[4] *Wenzhou Institute, University of Chinese Academy of Sciences, Wenzhou* 325001, *China*

(Received 8 January 2020; revised manuscript received 27 February 2020; accepted manuscript online 9 March 2020)

We quantify the mean potential energy of a passive colloidal particle harmonically confined in a bacterial solution using optical traps. We find that the average potential energy of the passive particle depends on the trap stiffness, in contrast to the equilibrium case where energy partition is independent of the external constraints. The constraint dependence of the mean potential energy originates from the fact that the persistent collisions between the passive particle and the active bacteria are influenced by the particle relaxation dynamics. Our experimental results are consistent with the Brownian dynamics simulations, and confirm the recent theoretical prediction.

Keywords: constraint dependence, average potential energy, active bath, passive tracer, optical trap

PACS: 82.70.Dd, 05.40.–a, 47.63.Gd **DOI:** 10.1088/1674-1056/ab7d9b

1. Introduction

Active matter systems, ranging from macroscopic scales including flocks of birds, shoals of fish to microscopic scales including swarming of bacteria, migrating cells, artificial colloidal particles, consist of self-propelling units that can convert ambient or stored energy into persistent motion.[1–17] Because of this unique property, active matter systems exhibit many unusual behaviors not found in passive systems, such as complex collective motions,[18–25] motility-induced phase separation,[26–28] or abnormal effective interactions.[29–32]

Recently, a growing effort has been devoted to exploring the statistical physics of passive particles immersed in an active bath.[29–38] In the system consisting of passive particles and active microswimmers, the swimmers produce non-thermal forces on the passive particle. Under the influence of the active fluctuations, a passive tracer in an active bath exhibits drastically different behaviors from a passive Brownian particle in a thermal bath.[39–41] Some fundamental thermodynamic quantities and relations are affected by the presence of the non-equilibrium fluctuations associated with the self-propulsions of the active particles. By generalizing the energy equipartition to the out-of-equilibrium systems, Claudio Maggi *et al.* proposed a theoretical formula for the average potential energy of a passive particle under a harmonic constraint in an active bath, and showed that the mean potential energy of the passive particle depends on the trap stiffness.[42] This scenario is fundamentally different from the equilibrium situation. Experimentally, however, no clear evidence of this constraint dependence has been reported, except measurement performed under a single constant constraint stiffness.

In this work, we experimentally study the dynamics of a passive particle optically trapped in a bacteria bath. The stiffness coefficient of the optical trap can be systematically varied by tuning the power of the optical tweezers. We first analyze the position distribution of the passive particle in the optical trap, which clearly deviates from the Boltzmann distribution in equilibrium state. Furthermore, the average potential energy of the passive particle is measured for different trap stiffness coefficients, and it shows a significant dependence on the trap stiffness, which agrees with the Brownian dynamics simulation and is consistent with the previous theoretical prediction. Our results also indicate that the energy equipartition cannot be trivially extended to the active systems.

2. Experimental method

E. coli bacteria (MG1655) with the length of ~ 2.5 μm and the diameter of ~ 0.6 μm are grown overnight at 37 ℃ on Luria–Bertani (LB) solid medium, after which the E.coli

*Project supported by the National Natural Science Foundation of China (Grant Nos. 11874397, 11674365, 11774393, and 11774394).
†There authors contributed equally to this work.
‡Corresponding author. E-mail: fye@iphy.ac.cn
§Corresponding author. E-mail: mcyang@iphy.ac.cn
¶Corresponding author. E-mail: kechen@iphy.ac.cn

bacteria are transferred from the solid medium to standard LB liquid medium (3 ml) and incubated for 4 h (37 ℃, 200 rpm shaker bath) to achieve strong activity with an averaged speed of ~ 20 μm/s. The polystyrene (PS) beads with the diameter of 3 μm are synthesized according to the method reported by Paine *et al.*[43] and stabilized by polyvinyl pyrrolidone. The E. coli bacteria dispersions are mixed with the PS bead solutions and loaded into a glass cell with a thickness of 30 μm. The dimensionless self-propelling force of the bacteria can be estimated as $\frac{F_d \sigma_s}{k_B T} = 19.3$, where F_d and σ_s are the self-propelling force and diameter of the bacteria, respectively. A PS particle is then randomly chosen and trapped by an optical tweezer near the upper glass surface (Fig. 1(a)), with low laser intensities so that the concentration and motility of the E. coli cells around the PS particle are not affected by the optical trap. To achieve high activity of the bacteria, the temperature of the glass cell is maintained at 37 ℃ by a resistive objective heater (Bioptechs). The PS particle experiences a confined active Brownian motion due to the combining effects of the thermal stochastic force and intermittent collisions from the bacteria. The images of the particles and bacteria are acquired on an inverted optical microscopy with a 100× magnification objective and recorded at 50 frames/s by a CCD camera (IDS uEye SE). A representative image of the PS particle constrained in the optical trap in the bacteria solution is shown in Fig. 1(b). Though the contour of the PS particle is slightly out of focus, the position of the particle can be precisely recognized as the center of the Gaussian light blob.

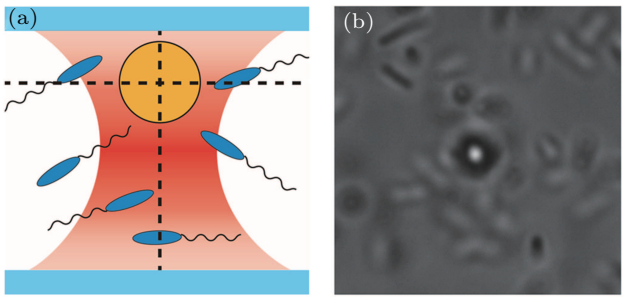

Fig. 1. (a) The schematic diagram of experiment system. The observing plane and center of optical trap are marked with dashed lines. (b) The image of PS particle optically trapped in a bacteria solution acquired by a 100× magnification objective.

The centroids of the PS particle are extracted using particle tracking techniques developed by Crocker and Grier.[44] In the linear response regime of the optical trap, the potential energy of beads equals to $\frac{1}{2}k\langle r^2\rangle$, where $\langle r^2\rangle$ is the mean square of the bead's displacement from the center of the trap and k is the stiffness coefficient of the optical trap. The mean potential energy U is taken over 10000 frames of particle positions in experiment. By tuning the laser power of the optical trap, we obtain the U as a function of k for various PS particle sizes and bacteria densities.

3. Calibration of the stiffness coefficient of the optical trap

The stiffness coefficient k depends on the laser intensity of the optical trap, and is calibrated by measuring the distribution of the trapped PS particle in the absence of bacteria. In thermal equilibrium, the displacement of the particle trapped in a harmonic potential is governed by a Boltzmann distribution

$$P(\boldsymbol{r}) \propto \exp\left(\frac{-U(\boldsymbol{r})}{k_B T}\right) = \exp\left(\frac{-k\boldsymbol{r}^2}{2k_B T}\right), \tag{1}$$

with k_B the Boltzmann constant. Figure 2(a) plots the particle position distribution with respect to the trap center in the x and y directions. The measured distribution can be well fitted with Eq. (1), from which the k can be extracted. Meanwhile, the perfect coincidence between the curves for two directions suggests that the strength of the optical trap is isotropic.

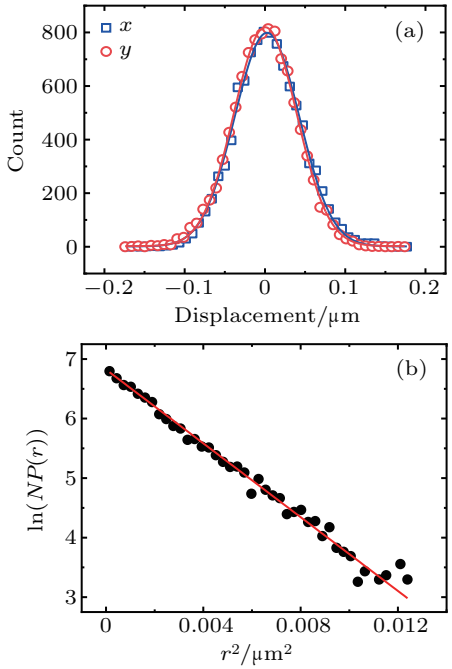

Fig. 2. (a) Position distribution of the passive particle in an optical trap in x and y directions without bacteria, where the extracted stiffness k is 2.65 pN/μm. Blue and red lines are fits with Eq. (1) for x and y directions, respectively. (b) Exponential fit (red line) of the radial position distribution measured in experiment (black circles) in a semi-log plot, where N is the total number of frames.

We can then plot the logarithmic radial position distribution as a function of $\boldsymbol{r}^2$ (Fig. 2(b)), where $NP(r)$ is the counting recorded near $\boldsymbol{r}$. The red line is the linear fit to the experiment data, and the slope of the red line corresponds to $\frac{-k}{2k_B T}$. Through the same procedure, we thus determine the trap stiffness coefficients for a series of different laser intensities.

4. Position distribution of the passive particle optically trapped in an active bath

We first compare the position distribution of an optically trapped passive particle in active and passive baths. The pas-

sive sample consists of a dead bacteria solution which is obtained by treating the bacteria with excessive ultraviolet rays, and it thus is in equilibrium state. Figure 3(a) plots the distribution of the passive particle along x axis under the constraint stiffness of 0.90 pN/μm. The range of movement of the passive particle is within $-0.60\ \mu\text{m} < x < 0.60\ \mu\text{m}$ in the active bath (red open squares) and $-0.30\ \mu\text{m} < x < 0.30\ \mu\text{m}$ for the passive case (blue open circles). The probability near the trap center ($x = 0.0\ \mu\text{m}$) in the active bath is lower than that in the passive case. The wider distribution of the passive particle trapped in the active bath than in the thermal bath is due to the fact that the passive particle can be pushed further away from the trap center due to the persistent collisions with the bacteria, compared to the case of the thermal bath. Similar results are also observed in the case where the constraint stiffness is 3.15 pN/μm in Fig. 3(b).

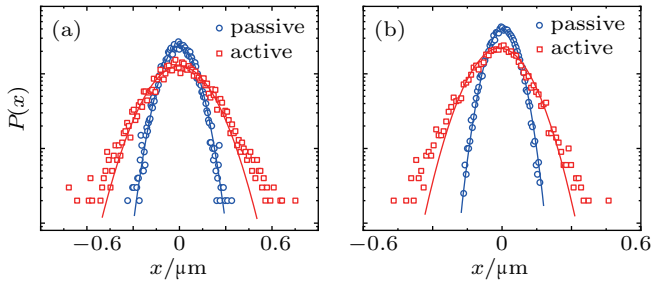

Fig. 3. Position distribution of the passive particle along x direction in an active bath (red open squares) and a passive bath (blue open circles) in an optical trap with constraint stiffness $k = 0.90$ pN/μm (a) and 3.15 pN/μm (b). Blue and red lines are fits with Gaussian functions. The packing fraction of bacteria is 0.032 and the size of the passive particle is 3 μm.

In thermal equilibrium, the distribution of a particle trapped in a harmonic potential can be fitted to a Gaussian function as presented in Eq. (1). For the trapped particle in a passive bath, we show that the particle distribution can indeed be well fitted to a Gaussian function, as plotted in Fig. 3 (blue lines). For the active bath, on the other hand, the particle distribution cannot be satisfactorily fitted to a Gaussian function, and deviates significantly at large displacements (red lines in Fig. 3). Such non-Gaussian distributions often exist for active systems, and have been observed in other experiments.[45,46] The non-Gaussian distribution of the particle positions originates from the persistent push from the bacteria. In particular, when the relaxation time of the harmonic trap τ_{trap} is shorter than the persistent time of the bacteria τ_{bac},[46] the bacteria can continuously push the passive particle to displacements not accessible to thermal fluctuations. Here τ_{trap} is given by the friction coefficient of the passive particle over constraint stiffness γ/k. In our experiments, τ_{trap} is estimated to be $\sim 10^{-2}$ s, shorter than τ_{bac} (~ 1 s). When $\tau_{\text{trap}} > \tau_{\text{bac}}$, the characteristic length of the tracer persistent motion induced by the active collisions from the bacteria is smaller than that of the optical trap, such that the trajectory of the tracer in a weak trap is Brownian-like but with a larger diffusion coefficient, thus the Gaussian distribution recovers.

5. The influence of constraint on the average potential energy of the passive particle

We explore the influence of constraint stiffness k on the average potential energy U by varying the stiffness coefficient of the optical trap. The measured average potential energy U as a function of k for various bacterial packing fractions ρ is plotted in Fig. 4(a). Here, U and k are nondimensionalized by the system parameters as $U/k_{\text{B}}T$ and $k\sigma_{\text{s}}^2/k_{\text{B}}T$, respectively. As plotted in Fig. 4(a), for all the concentrations of bacteria ($\rho = 0.017$, 0.032, and 0.050), the average potential energy of the passive particle exceeds the equilibrium value of $k_{\text{B}}T$, as the bacteria can push the trapped PS particle to larger displacements as shown in Fig. 3. For a given concentration, the potential energy of the trapped particle decreases with the trap stiffness k. For comparison, we measure the potential energy in the samples with dead bacteria treated by ultraviolet rays (passive curve in Fig. 4(a)), and U nearly remains unchanged with the increase of k. The potential energy obtained in the passive bath is still slightly above $k_{\text{B}}T$, as a few bacteria survive the ultraviolet treatment and slightly contribute to the additional potential energy of the PS particle. For the whole range of k in Fig. 4(a), U increases with ρ, as higher concentration of active swimmers enhances the collision frequency between the particle and active swimmers, thus strengthens the overall active force exerted on the passive particle. The above results clearly indicate that the average potential energy of a passive particle in an active bath strongly depends on the constraint, significantly different from the case of a thermal bath in which U is constant and is independent of external constraints.

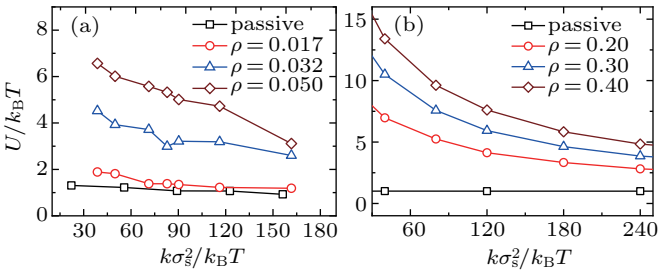

Fig. 4. The average potential energy $U/k_{\text{B}}T$ as a function of external constraint $k\sigma_{\text{s}}^2/k_{\text{B}}T$ for various bacterial packing fractions ρ in experiment (a) and simulation (b). The particle size is $5\sigma_{\text{s}}$ in (a) and $3\sigma_{\text{s}}$ in (b). The passive curves correspond to the inactive bacteria sample.

The constraint-dependence of the average potential energy in an active bath is verified by Brownian dynamics simulations. The simulation system consists of one large passive particle constrained in a harmonic trap and 2000 small self-propelling active Brownian particles. The dimensionless self-propelling force of the active particles is taken as $\frac{F_{\text{d}}\sigma_{\text{s}}}{k_{\text{B}}T} = 20$,

comparable to the bacteria in the experiments. The orientation of the active particle evolves according to rotational diffusion, while the rotational degree of freedom of the passive tracer is not taken into account. Figure 4(b) plots U/k_BT as a function of $k\sigma_s^2/k_BT$, and different curves represent different packing fractions of the active swimmers. The passive case, where the self-propelling force of the active particles is switched off, is also plotted for comparison. In agreement with the observations in experiment, the average potential energy of the passive sphere in the simulations also decreases with the trap constraint, and remains higher than k_BT. The relatively larger concentrations of the active swimmers in simulations ($\rho = 0.20$, 0.30, and 0.40) than in experiments ($\rho = 0.017$, 0.032, and 0.050) is due to the fact that the simulation is performed in a purely two-dimensional (2D) system, while the experimental system is three-dimensional (3D). For the experiments, an effective 2D concentration can be estimated by considering the 3D collisions from the active swimmers. The effective concentration thus obtained is comparable to that in the simulations.

The dependence of the average potential energy on constraint in the active systems can be explained by the active interactions between the passive particle and surrounding active swimmers. When colliding with the swimmer, the passive particle may reach a maximum deviation from the trap center, $\Delta r = \boldsymbol{F}/k$, where the friction vanishes. Due to force balance between $\boldsymbol{F}$ and the restoring force from the trap, the active contribution to the average potential energy can be estimated as $\frac{1}{2}k\Delta r^2 = \boldsymbol{F}^2/2k$, inversely proportional to the trap stiffness coefficient. The total mean potential is thus $k_BT + \boldsymbol{F}^2/2k$. Note that this simple picture is valid for large k, otherwise the bacteria may reorientate and swim away before reaching the maximum displacements. Following Ref. [42], the average potential energy of the passive particle harmonically trapped in an active bath can be calculated by

$$U(k) = k_BT + \frac{A}{1+Bk}, \tag{2}$$

where the second term $\frac{A}{1+Bk}$ results from the active noise, and A and B are the parameters of the active noise. The theoretical formula illustrates that the active contribution to the potential energy is inversely proportional to the constraint stiffness k, which is consistent with our intuitive explanation above.

In equilibrium, the potential energy of a tracer particle is independent of the mass or the size of the particle. In the active bath, we show that the average potential energy also depends on the size ratio between the passive tracer and the active swimmers. Figure 5(a) plots the potential energy of the PS particles of different sizes in the bacteria solution with packing fraction $\rho = 0.05$. The potential energy U increases with the particle size. Similar trend is recovered in simulations with tracers of different diameters. The dependence of the potential energy on the particle size is explained as follows. Particles with larger interaction areas can simultaneously collide with more bacteria, which on average exert greater forces on the passive particle. Under the persistent push of more bacteria, larger particles can deviate farther from the optical center, thus have greater potential energy, under the same trap stiffness.

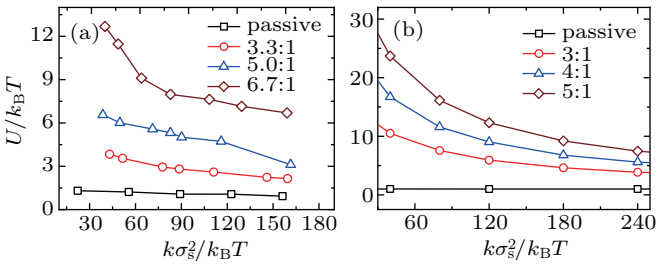

Fig. 5. The average potential energy U/k_BT as a function of external constraint $k\sigma_s^2/k_BT$ for various particle sizes in experiment (a) and simulation (b). ρ is 0.050 for (a) and 0.30 for (b).

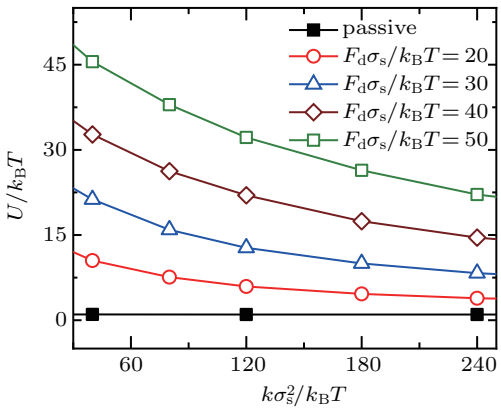

Fig. 6. The average potential energy of the passive tracer U/k_BT as a function of external constraint $k\sigma_s^2/k_BT$ for various self-propelled force $\frac{F_d\sigma_s}{k_BT}$ in simulation. The particle size ratio is 3:1 and the packing fraction ρ is 0.30.

We finally perform simulation to explore the constraint dependence of the average potential energy for various driving forces of the active swimmers. As plotted in Fig. 6, for all the driving forces ($\frac{F_d\sigma_s}{k_BT} = 20$, 30, 40, and 50), the constraint-dependent mean potential energies are found, compared with the passive case ($\frac{F_d\sigma_s}{k_BT} = 0$). In addition, the potential energy increases with the driving force, as a result of enhancement of the interaction between the passive tracer and active swimmers.

6. Conclusion

We measure the average potential energy of a passive particle in an active bath using optical trap experiments and computer simulations. We find that the average potential energy of a trapped tracer particle clearly deviates from the energy equi-partition theorem in the equilibrium case. The potential energy decreases with trap stiffness, while remains above k_BT. The distribution of the particle position in an active bath

exhibits non-Gaussian characteristics, with wider range than the equilibrium case, thus indicating higher potential energy. The measured potential energy increases with the concentration and driving force of the active swimmers, and the size of the passive particle. The inverse dependence of the potential energy on the trap stiffness can be qualitatively understood by the force balance between the persistent self-propelling force of the active swimmers and the restoring force of the trap. Our results thus provide unambiguous experimental and simulation evidences for previous theoretical prediction.

Acknowledgments

We thank Y. Zong for the synthesis of the PS colloidal microspheres and providing the bacterial strain. We also thank R. Liu for helpful discussions.

References

[1] Ramaswamy S 2010 *Annu. Rev. Condens. Matter Phys.* **1** 323
[2] Marchetti M C, Joanny J F, Ramaswamy S, Liverpool T B, Prost J, Rao M and Simha R A 2013 *Rev. Mod. Phys.* **85** 1143
[3] Di Leonardo R, Angelani L, Dell'Arciprete D, Ruocco G, Iebba V, Schippa S, Conte M P, Mecarini F, De Angelis F and Di Fabrizio E 2010 *Proc. Natl. Acad. Sci. USA* **107** 9541
[4] Jiang H R, Yoshinaga N and Sano M 2010 *Phys. Rev. Lett.* **105** 268302
[5] Maggi C, Saglimbeni F, Dipalo M, De Angelis F and Di Leonardo R 2015 *Nat. Commun.* **6** 7855
[6] Palacci J, Sacanna S, Steinberg A P, Pine D J and Chaikin P M 2013 *Science* **339** 936
[7] Catchmark J M, Subramanian S and Sen A 2005 *Small* **1** 202
[8] Paxton W F, Kistler K C, Olmeda C C, Sen A, St. Angelo S K, Cao Y, Mallouk T E, Lammert P E and Crespi V H 2004 *J. Am. Chem. Soc.* **126** 13424
[9] Gangwal S, Cayre O J, Bazant M Z and Velev O D 2008 *Phys. Rev. Lett.* **100** 058302
[10] Theurkauff I, Cottin-bizonne C, Palacci J, Yber C and Bocquet L 2012 *Phys. Rev. Lett.* **108** 268303
[11] Zhang H P, Be'er A, Florin E L and Swinney H L 2010 *Proc. Natl. Acad. Sci. USA.* **107** 13626
[12] Wioland H, Woodhouse F G, Dunkel J, Kessler J O and Goldstein R E 2013 *Phys. Rev. Lett.* **110** 268102
[13] Sokolov A and Aranson I S 2012 *Phys. Rev. Lett.* **109** 248109
[14] Sokolov A, Aranson I S, Kessler J O and Goldstein R E 2007 *Phys. Rev. Lett.* **98** 158102
[15] Yang M, Ripoll M and Chen K 2015 *J. Chem. Phys.* **142** 054902
[16] Dey K K, Zhao X, Tansi B M, Méndez-Ortiz W J, Córdova-Figueroa U M, Golestanian R and Sen A 2015 *Nano Lett.* **15** 8311
[17] Zong Y, Liu J, Liu R, Guo H, Yang M, Li Z and Chen K 2015 *ACS Nano* **9** 10844
[18] Vicsek T and Zafeiris A 2012 *Phys. Rep.* **517** 71
[19] Elgeti J, Winkler R G and Gompper G 2015 *Rep. Prog. Phys.* **78** 056601
[20] Deblais A, Barois T, Guerin T, Delville P H, Vaudaine R, Lintuvuori J S, Boudet J F, Baret J C and Kellay H 2018 *Phys. Rev. Lett.* **120** 188002
[21] Kokot G, Das S, Winkler R G, Gompper G, Aranson I S and Snezhko A 2017 *Proc. Natl. Acad. Sci. USA* **114** 12870
[22] Bricard A, Caussin J B, Desreumaux N, Dauchot O and Bartolo D 2013 *Nature* **503** 95
[23] Yan J, Han M, Zhang J, Xu C, Luijten E and Granick S 2016 *Nat. Mater.* **15** 1095
[24] Massana-Cid H, Meng F, Matsunaga D, Golestanian R and Tierno P 2019 *Nat. Commun.* **10** 2444
[25] Wensink H H, Dunkel J, Heidenreich S, Drescher K, Goldstein R E, Löwen H and Yeomans J M 2012 *Proc. Natl. Acad. Sci. USA* **109** 14308
[26] Buttinoni I, Bialké J, Kümmel F, Löwen H, Bechinger C and Speck T 2013 *Phys. Rev. Lett.* **110** 238301
[27] Cates M E and Tailleur J 2015 *Annu. Rev. Condens. Matter Phys.* **6** 219
[28] Sesé-Sansa E, Pagonabarraga I and Levis D 2018 *Europhys. Lett.* **124** 30004
[29] Angelani L, Maggi C, Bernardini M L, Rizzo A and Di Leonardo R 2011 *Phys. Rev. Lett.* **107** 138302
[30] Ni R, Stuart M A C and Bolhuis P G 2015 *Phys. Rev. Lett.* **114** 018302
[31] Yamchi M Z and Naji A 2017 *J. Chem. Phys.* **147** 194901
[32] Ray D, Reichhardt C and Olson Reichhardt C J 2014 *Phys. Rev. E* **90** 013019
[33] Dolai P, Simha A and Mishra S 2018 *Soft Matter* **14** 6137
[34] Angelani L 2019 *J. Phys.-Condes. Matter* **31** 075101
[35] Takatori S C and Brady J F 2015 *Soft Matter* **11** 7920
[36] Stenhammar J, Wittkowski R, Marenduzzo D and Cates M E 2015 *Phys. Rev. Lett.* **114** 018301
[37] Loi D, Mossa S and Cugliandolo L F 2008 *Phys. Rev. E* **77** 051111
[38] Loi D, Mossa S and Cugliandolo L F 2011 *Soft Matter* **7** 3726
[39] Bechinger C, Di Leolardo R, Löwen H, Reichhardt C, Volpe G and Volpe G 2016 *Rev. Mod. Phys.* **88** 045006
[40] Peng Y, Lai L, Tai Y S, Zhang K, Xu X and Cheng X 2016 *Phys. Rev. Lett.* **116** 068303
[41] Wu X L and Libchaber A 2000 *Phys. Rev. Lett.* **84** 3017
[42] Maggi C, Paoluzzi M, Pellicciotta N, Lepore A, Angelani L and Di Leonardo R 2014 *Phys. Rev. Lett.* **113** 238303
[43] Paine A J, Luymes W and McNulty J 1990 *Macromolecules* **23** 3104
[44] Crocker J C and Grier D G 1996 *J. Colloid Interface Sci.* **179** 298
[45] Krishnamurthy S, Ghosh S, Chatterji D, Ganapathy R and Sood A K 2016 *Nat. Phys.* **12** 1134
[46] Argun A, Moradi A R , Pinçe E, Bagci G B, Imparato A and Volpe G 2016 *Phys. Rev. E* **94** 062150